Smart Structures and Systems, *Vol. 21, No. 1 (2018) 27-35*
DOI: https://doi.org/10.12989/sss.2018.21.1.027

BOTDA based water-filling and preloading test of spiral case structure

Heliang Cui[1,2], Dan Zhang*[1], Bin Shi**[1] and Shusheng Peng[3]

[1]*School of Earth Sciences and Engineering, Nanjing University, Nanjing 210023, China*
[2]*POWERCHINA Huadong Engineering Corporation Limited, Hangzhou 311222, China*
[3]*Zhejiang Huadong Engineering Safety Technology Co.,Ltd., Hangzhou 311222, China*

(Received July 30, 2017, Revised December 3, 2017, Accepted December 13, 2017)

Abstract. In the water-filling and preloading test, the sensing cables were installed on the surface of steel spiral case and in the surrounding concrete to monitor the strain distribution of several cross-sections by using Brillouin Optical Time Domain Analysis (BOTDA), a kind of distributed optical fiber sensing (DOFS) technology. The average hoop strain of the spiral case was about 330 με and 590 με when the water-filling pressure in the spiral case was 2.6 MPa and 4.1 MPa. The difference between the measured and the calculated strain was only about 50 με. It was the first time that the stress adjustment of the spiral case was monitored by the sensing cable when the pressure was increased to 1 MPa and the residual strain of 20 με was obtained after preloading. Meanwhile, the shrinkage of 70 ~ 100 με of the surrounding concrete was effectively monitored during the depressurization. It is estimated that the width of the gap between the steel spiral case and the surrounding concrete was 0.51 ~ 0.75 mm. BOTDA based distributed optical fiber sensing technology can obtain continuous strain of the structure and it is more reliable than traditional point sensor. The strain distribution obtained by BOTDA provides strong support for the design and optimization of the spiral case structure.

Keywords: BOTDA; distributed optical fiber sensing; strain distribution; spiral case; water-filling; preloading; hydraulic structure

1. Introduction

JinPing-II hydropower station, which is mainly composed of a gate dam and 4 diversion tunnels, is located at Liangshan region, Sichuan province of China. JinPing-II cuts Yalong river to get 310 m water head for 4800 MW installed capacity. In this project, the greatest tunnel group in the world was built with the features of deep (2525 m deepest), long (16.7 km average) and large (12.4~14.6 m diameter) (Zhang *et al.* 2011). Many engineering problems were encountered during construction because of its huge scale, high overburden and complex geological conditions.

JinPing-II is equipped with 8 francis turbine units, each of which generates a capacity of 600 MW. The rated and maximum hydrostatic head of the generators are 288 m and 329.2 m. The spiral cases were installed to take the maximum water pressure of 4.04 MPa. The cross-section diameter of spiral case inlet is 6.05m and the thickness of steel shell is 30~70 mm. Preloading pressure of 2.6 MPa was taken according to the calculation.

The surrounding concrete was casted and harden with a stable preloading pressure of 2.6 MPa inside the spiral case. The concrete structure can share stress when water pressure exceeds the preloading value during operation. The preloading spiral case is suited for large/medium hydropower plant and pumped storage power station with high hydraulic head and large capacity, which requires higher stabilization and better vibration resistance. Appropriate preloading pressure is important for restraining the vibration of spiral case, adjusting the stress of steel shell, as well as controlling the gap width between spiral steel case and surrounding concrete for optimal stress bearing ratio. For previous projects and researches, the design mainly depended on numerical simulation and experiences. The data measured during preloading process were seldom used for design feedback. Generally, a large hydropower station will select 2 spiral cases for safety monitoring, the purposes of which are: (1) to inspect installation quality of the spiral case; (2) to monitor and analyze the safety status of the steel shell and the concrete structure during the construction; (3) to evaluate the operation status of the spiral case as well as the hydropower station. There were some point sensors, such as strain/stress/displacement gauges which has been used for structural health monitoring. However, these traditional sensors are inadequate to monitor such a geometrically complicated spiral case because of large quantity of point sensors needed and difficulty of installation. It is hardly to obtain data with high quality and to interpretate the results in a convincing way, e.g. to get displacement by integration with the sparse point data (Ding 2011, Xue *et al.* 2012).

Brillouin Optical Time Domain Analysis (BOTDA) is a distributed optical fiber sensing (DOFS) technology based on stimulated Brillouin scattering in an optic fiber, which is able to measure the strain and temperature distribution

*Corresponding author, Associate Professor
E-mail: zhangdan@nju.edu.cn
**Professor
E-mail: shibin@nju.edu.cn

http://www.techno-press.com/journals/sss&subpage=7 ISSN: 1738-1584 (Print), 1738-1991 (Online)

along an optical fiber over kilometers or tens of kilometers and has been used in structure health monitoring for tunnels, bridges and other civil structures (Shi *et al.* 2011, Li *et al.* 2015, Liu *et al.* 2015, Soga *et al.* 2015). With recent development of the demodulation instruments, shorter spatial resolution and higher precision have been achieved, and then the application range has been extend to the monitoring of small structural defections, such as cracks and local deformation (Yamauchi *et al.* 2007, Bao *et al.* 2016).

In this paper, BOTDA was utilized to monitor the strain distribution of spiral steel case in the process of water-filling, in which the water pressure was increased to 4.1 MPa and then decreased to zero. Afterwards, the strain distribution of the spiral case and that of the surrounding concrete were monitored in the process of preloading with water pressure of 2.6 MPa. The continuous strain data obtained by BOTDA can be used to evaluate structural deformation, stress state and bearing ratio of preloading spiral case, which is helpful for design optimization and safety assessment. It is the first application of BOTDA for spiral case, which is significant for the development of DOFS as well as the structural health monitoring of large hydraulic project.

2. Monitoring design of spiral case

2.1 BOTDA

By using OTDR or OFDR, temperature and strain along the optical fiber can be detected according to the intensity or frequency change of scattered light in the optical fiber (Bao and Chen 2012). Brillouin scattering was derived by the inelastic collision of acoustic wave and light wave propagating inside optical fiber. If temperature or axial strain of the optical fiber changes, the frequency of the Brillouin scattering will shift, which keeps a linear relationship with strain or temperature change (Culverhouse *et al.* 1989, Horiguchi *et al*. 1989). Based on the above principles, BOTDA was invented to measure strain and temperature distribution along an optical fiber simultaneously by one scanning, during which Stimulated Brillouin Scattering (SBS) is detected and analyzed when pulse pump laser and continuous probe laser are injected from both ends of the fiber.

In 1999, commercial BOTDA strain analyzer was developed and then applied for qualitative or global monitoring of large scale structure with 50 με repeatability and 1m spatial resolution (SR). Pulse Pre-Pump BOTDA (PPP-BOTDA) was developed to improve the performance of 10 με repeatability with 0.1m SR in 2004 (Kishida *et al.* 2004). And then, the measurement time was shortened to tens of seconds (Li *et al*. 2008), which extended the engineering applications of BOTDA greatly and made precise monitoring possible.

With the consideration of monitoring requirements of spiral case structure on sampling time, accuracy, SR, *et al.*, NBX-6050, a type of PPP-BOTDA was selected in this study. The performance of NBX-6050 was verified by two tests: i) 0.1 m SR by Dissimilar-Fiber-Splicing calibration method (Zhang *et al.* 2013); ii) 10 με repeatability by continuous testing of a naked fiber inside the mixture of ice and water. Finally, the measuring parameters of NBX-6050 were determined as follows: 1ns pulse width, 500 m measuring range, 10,000 total sampling point, 0.05 m sampling point spacing, 2 MHz frequency scanning step, 2^{15} averaging times and 1.5 min sampling time. The actual repeatability of the monitoring approach was 20~30 με, which was influenced mainly by length and quality of the sensing cable.

2.2 Strain sensing cable

An important part of the whole monitoring system is the sensing cable, which is composed of core, cladding, coating, jacket and other reinforcements. Compared with the communication cable, the strain sensing cable has a different package design. In particular, some performance and factors need be considered in the selection and development of strain sensing cables, such as installation method, damage resistance, durability, initial strain state, deformation coordination, temperature coefficient and waterproof capacity. The reasonable package and protection methods depend on the requirements of engineering applications.

Two kinds of sensing cable were adopted for the monitoring of spiral case structure. One is the strain sensing cable with metal tape packaging (model: NZS-DSS), which was glued on the surface of the spiral case for strain monitoring of steel structure. The other is the reinforced embedded strain sensing cable (model: NZ-GFRP), which was implanted in the surrounding concrete for strain monitoring of concrete structure. The reinforced embedded strain sensing cable has a relative good performance under long-term stress and cyclic loading (Zhang *et al*. 2016). The two sensing cables are shown in Fig. 1 and the main parameters are shown in Table 1.

The strain coefficient of the fiber core is 0.051 MHz/με and the temperature coefficient is about 1 MHz/℃ according to the calibration experiments. As the spiral case was built in the deep rock mess, the ambient temperature change was very small. Therefore, temperature compensation for the strain sensing cable can be ignored during the test.

Table 1 Parameters of two sensing cables

Parameters	NZS-DSS	NZ-GFRP
Cross-section	Flat	Round
Cross-section size (mm)	15×0.15	φ6
Fiber type	Single mode	Single mode
Number of fibers	2	1
Elastic Modulus (GPa)	3~5	30
Tensile strength (N)	>800	>800

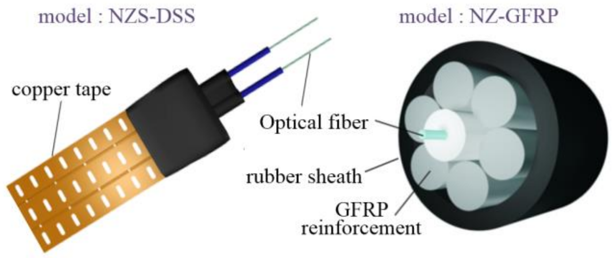

Fig. 1 Structure of strain sensing cables

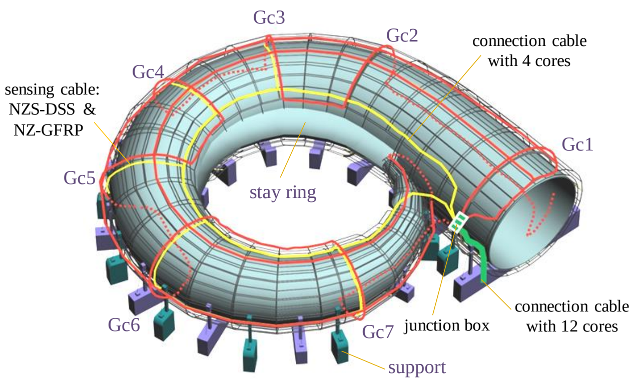

Fig. 2 Layout of sensing cables on spiral case

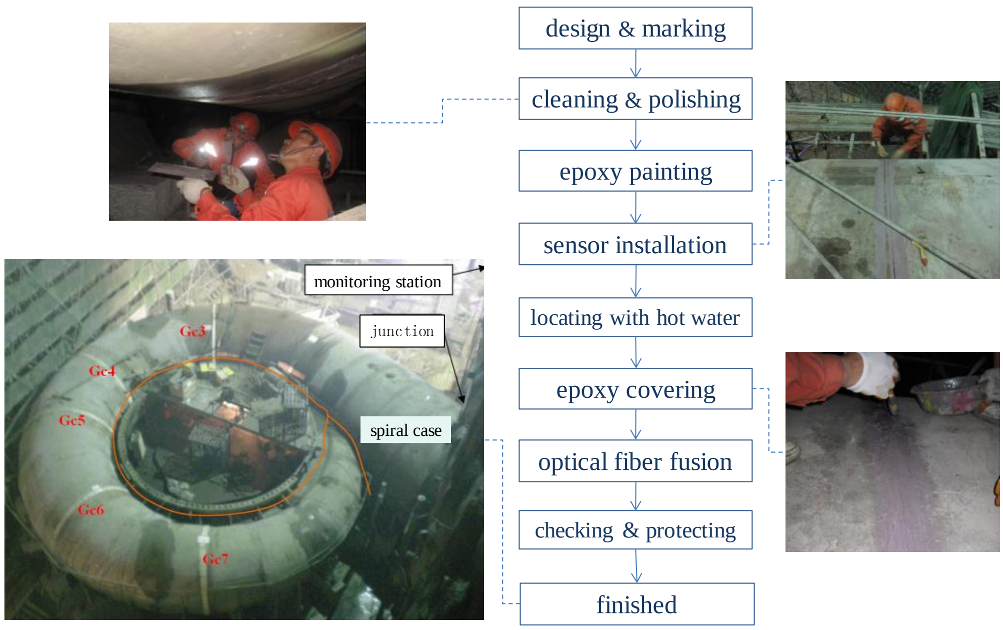

Fig. 3 Installation process of sensing cable on the surface of spiral case

2.3 Installation of sensing cable

The experiment was conducted on the spiral case of turbine unit 4# in JinPing-II hydropower station. Seven typical hoop cross-sections on the spiral case structure were selected for strain/stress monitoring. In each cross-section, the sensing cables were installed in C-shape on the outer surface of the spiral steel case and along the rebar of the surrounding concrete from the bottom to the top of the case, as shown in Fig. 2. For comparison, some traditional point sensors including steel plate stress meters, reinforcement stress gauges, strain gauges were installed on upstream side

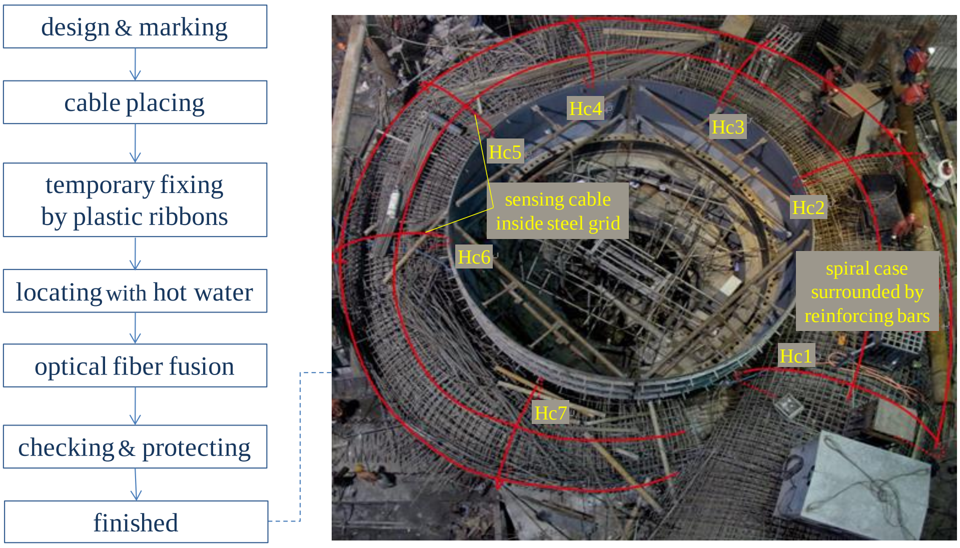

Fig. 4 Installation process of sensing cable in the surrounding reinforcement cage

of Gc3, downstream side of Gc4 as well as the middle cross-section between Gc6 and Gc7. The accuracy of stress meter and reinforcement stress gauge is 0.1%F.S. The accuracy of strain gauge is ± 5με.

The installation process of the NZS-DSS sensing cable on the spiral case surface is shown in Fig. 3. According to the monitoring design, the installation location was marked on the spiral case. Before the installation, it is necessary to clear and polish the installation location and paint the bottom glue with epoxy on the surface of spiral case. In order to match the sensing points of the cable with the monitoring location of the structure, we designedly increase the temperature of the optical cable at certain location with hot water so that an obvious signal change can be found on the strain curve at certain length of cable. And then the sensing cable was covered with epoxy followed by optical fiber fusion, cable checking and protecting to finish the cable installation.

Before the preloading, the reinforced cage was assembled around the spiral case. NZS-GFRP reinforced embedded strain sensing cable was laid along the rebar to monitor the strain distribution of concrete structure. The installation process of sensing cable are shown in Fig. 4.

The cross-sections in the concrete were named from Hc1~Hc7.

3. Strain distribution and variation of spiral steel case during Water-filling test

3.1 Hoop strain distribution

Water-filling test was carried out in the spiral case for 350 minutes and the water pressure was increased to 4.1 MPa step by step. The strain distribution before loading (0 MPa) was taken as the reference value to calculate the strain changes under different loads. The measurement of Gc4 and Gc6 cross-sections are shown in Fig. 5. The results of other cross-sections were similar to those of Gc4 and Gc6. The spiral case was assembled with the top, mid and bottom pieces, which made the strain of the C-shape cross-section have segmented distribution and following characteristics:

- The hoop strain distribution in a single piece was uniform.
- The strain of the top and bottom pieces was very close whereas the strain of the mid piece was slightly larger.
- Due to step-like surface of the welding, the sensing cable may not be tightly glued on the surface of the spiral case. The stress around the welds was complicated, which results in a significant small strain of the sensing cable.

3.2 Strain variation at typical locations

Three typical locations on top, mid and bottom piece were selected respectively to reveal the strain variation during the loading, as shown in Fig. 6.

When the water pressure was 2.6 MPa, the hoop strains of the top and bottom pieces were 330 με and 321 με, and they were 544 με and 522 με under the pressure of 4.1 MPa. The hoop strain of the mid piece was slightly larger. When the pressure were 2.6 MPa and 4.1 MPa, the hoop strains at mid surface were 410 με and 670 με respectively.

When the pressure was the same either at loading stage or unloading stage, the measured strain kept almost consistent. For example, when the pressure decreased to 2.6 MPa, the strain difference between the loading and unloading stage were +40, -7 and +9 με. When the pressure decreased to 0 MPa, the strain difference were -25, -14 and -22 με compared with the initial strain before the water-filling test.

During the loading stage, there was an inflection point for the slope of strain/pressure. When the pressure was less than 1 MPa, the slopes of strain/pressure at mid, top and bottom location were 112, 86 and 97 με/MPa. When pressure was more than 1 MPa, the slopes increased to 181,

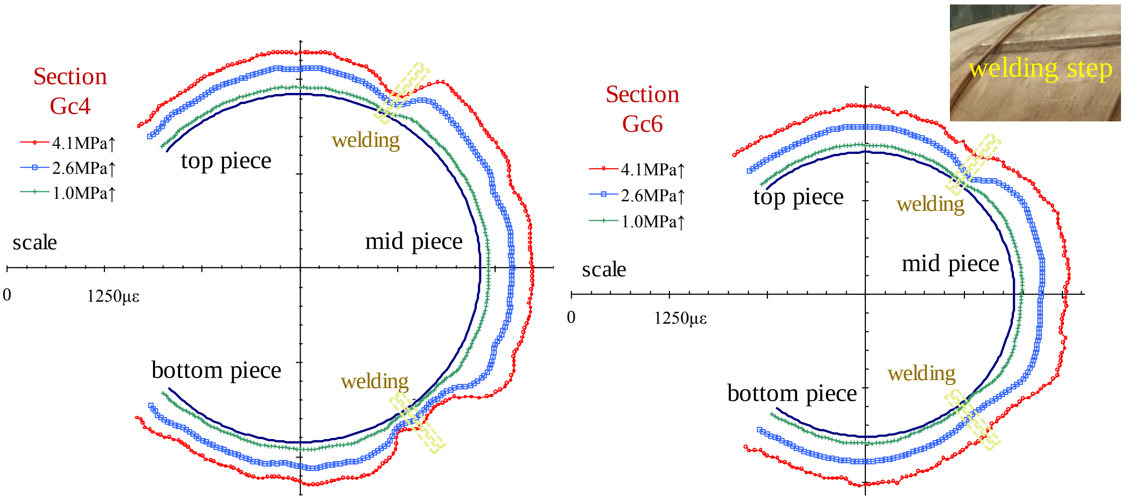

Fig. 5 Hoop strain distribution on the surface of spiral steel case

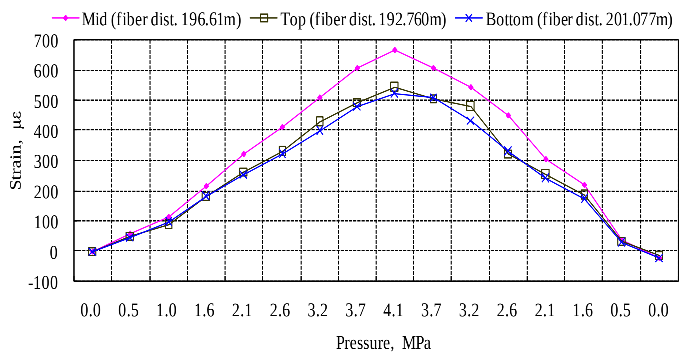

Fig. 6 Cable strain vs. water pressure at typical locations of Gc4 cross-section

148 and 138 με/MPa respectively. However, the inflection point during the unloading stage was not obvious. The slopes were 176, 144 and 142 με/MPa, which were close to those of loading stage when the pressure was more than 1 MPa.

4. Strain comparison of the spiral steel case

4.1 Theoretical and numerical models

Regarded as a closed pressure pipe, the hoop stress σ_c and longitudinal stress σ_L of the spiral case was calculated by

$$\sigma_c = \frac{rp}{t}\frac{r_c + r_{sp}}{2r_{sp}} \tag{1}$$

$$\sigma_L = \frac{rp}{2t} \tag{2}$$

where r_c is the distance from center of hoop pieces to structural center line of spiral case (mm); r_{sp} is the distance from calculating point to structural center line (mm); r is the radius of spiral case (mm); t is the thickness of spiral case (mm); p is the water pressure (MPa).

Sensing cables were attached onto the spiral case surface where the radial stress σ_r is 0. According to Hooke's law, hoop strain ε_c and longitudinal strain ε_L are

$$\varepsilon_c = \frac{1}{E}(\sigma_c - \mu\sigma_L) \tag{3}$$

$$\varepsilon_L = \frac{1}{E}(\sigma_L - \mu\sigma_c) \tag{4}$$

The spiral case was made of S500M low-alloy and high strength steel whose Young's modulus E equals to 205 GPa, and Poisson's ratio μ equals to 0.3.

ANSYS was applied to establish a three-dimensional FEM model of the spiral case and linear elasticity numerical simulation was conducted. Hexahedral element was adopted for meshing. For Gc4 cross-section, there were 294342 nodes and 238794 elements. As to the water-filling test, it is

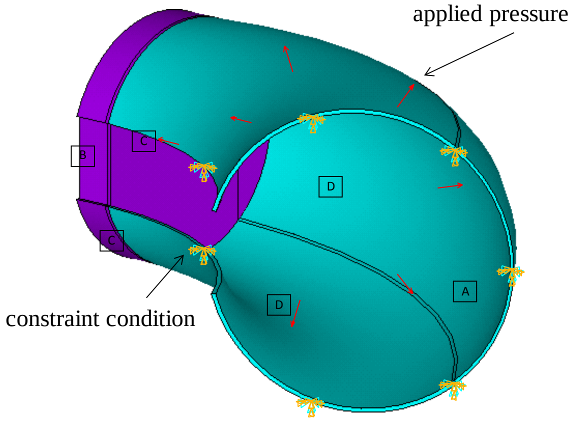

Fig. 7 FEM model of Gc4 cross-section

Table 2 Comparison between the measured and calculated strain (unit: με)

Water pressure / Cross-sections		2.6 MPa				4.1 MPa			
		Gc3	Gc4	Gc6	Gc7	Gc3	Gc4	Gc6	Gc7
Eq.*	top/bottom	380	382	395	402	599	603	623	634
	mid	429	431	429	423	676	679	676	667
Sim.	top/bottom	398	395	393	402	628	622	620	634
	mid	409	406	404	406	646	641	637	640
FOS	top/bottom	360/270	330/321	338/333	342/258	*none*	544/522	614/626	536/500
	mid	302	410	358	352	*none*	666	673	626
Gag.	top/bottom	371/121	390/246	414/*Err*	*none*	606/*Err*	650/406	683/*Err*	*none*
	mid	500	128	144	*none*	*Err*	219	249	*none*

*Eq.: theoretical formula; Sim.: numerical simulation; FOS: sensing cable; Gag.: steel plate stress meter

not necessary to consider other factors except the constraint condition of the stay ring and water pressure changes within the spiral case. FEM model of Gc4 is shown in Fig.7. The constraint conditions were represented by A, B, C and D respectively. A was the fixed constraint on the upstream side. B was used to simulate the spiral case on the downstream side, whose thickness is 600 mm and Young's modulus equals to 2050 GPa. C represented the fixed constrain of the stay ring. The water-filling pressure applied on the inner surface of spiral case was denoted by D.

4.2 Comparison with other methods

The parameters were the same in theoretical analysis and numerical simulation. The effects of supports on the bottom of spiral case was not taken into account. Therefore, the stress and strain on the top and bottom piece were equal because the pressure applied on the spiral case was symmetrical. The calculation results and the measured strain by sensing cables are listed in Table 2 when the water-filling pressures were 2.6 MPa and 4.1 MPa.

The theoretical and numerical results were close to each other except the strain on the mid piece, where the theoretical strain was slightly larger than that of numerical simulation. Besides a few sensing points, the strain measured by sensing cable was similar to, but slightly less than about 10% of the calculated value generally. The deviation between the sensing strain and calculated strain was due to the simplified boundary conditions in numerical simulation, such as the bottom supports of the spiral case. Especially at the bottom of cross-sections Gc3 and Gc7, the cable strain was 100 με smaller than that on the top at the pressure of 2.6 MPa.

A total of 12 steel plate stress meters were mounted on the top, mid and bottom surface of the spiral case in four monitoring cross-sections, three of which were close to Gc3,

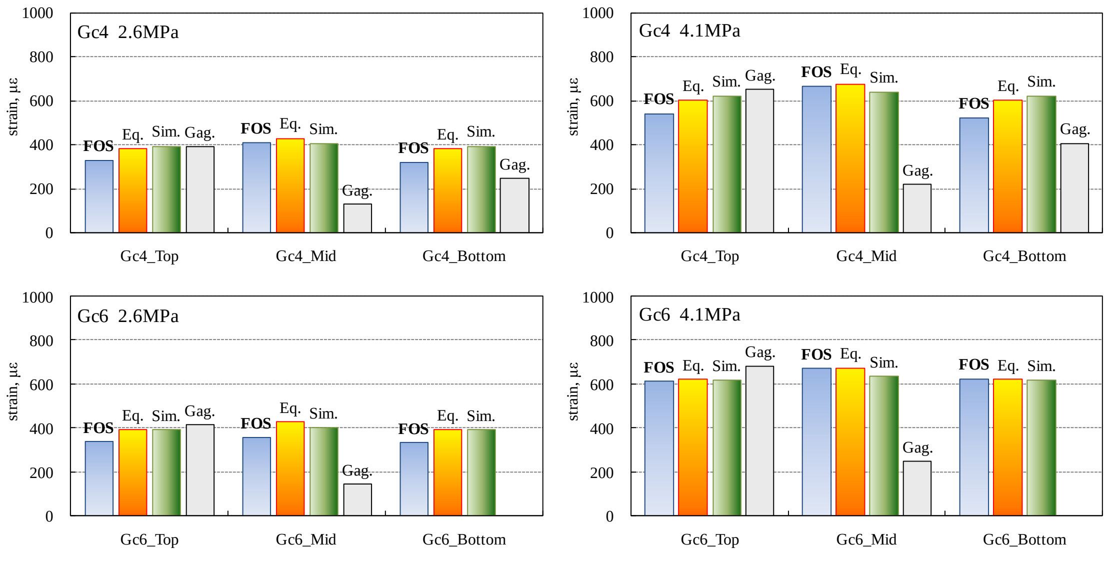

Fig. 8 Strain comparison of Gc4 and Gc6 cross-sections

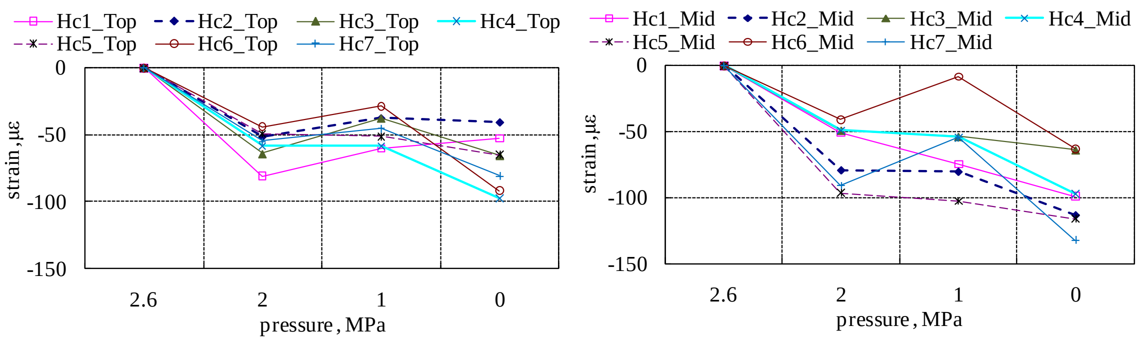

Fig. 9 Strain at typical location of surrounding concrete

Gc4 and Gc6, respectively. The results of steel plate stress meters are shown in Table 2. When the water pressure was 2.6 MPa and 4.1 MPa, a comparison between the strains of sensing cable (FOS), theoretical formula (Eq.), numerical simulation (Sim.) and steel plate stress meter (Gag.) is shown in Fig. 8.

During the field installation, it is difficult to control the installation direction and coupling with the spiral case because of the curved surface of the spiral case. The data obtained by the steel plate stress meters on the top piece were relatively good, whereas the measured data of the mid and bottom pieces were relatively poor. In addition, some steel plate stress meters on the mid and bottom pieces were out of work.

In contrast, the reliability of the sensing cable was high. And more importantly, the strain distribution of the whole cross-section of spiral cross-section can be obtained, which shows the superiority of the BOTDA technology. At present, there is no other reports about the field monitoring which can accurately and completely obtain the strain distribution and its changes during the water-filling test.

5. Strain distribution and its variation of surrounding concrete during preloading

5.1 Strain measured by sensing cable

After the water-filling with a cycle of loading and unloading, the water pressure was increased again and kept at 2.6 MPa for preloading test. With the pressure of 2.6 MPa, reinforcement cage was assembled and concrete was poured to construct the surrounding concrete structure. After the concrete reached its strength, the water pressure of the spiral case was released slowly for 120 min, among which the sustaining time for pressure of 2 MPa and 1 MPa was about 20 min respectively.

During the process of unloading, the strain variations of surrounding concrete on all cross-section were similar. The strain variation on the top and mid piece of each cross-section is shown in Fig. 9.

When the water pressure decreased from 2.6 MPa to 2.0 MPa, the spiral case contracted and separated from the surrounding concrete. The apparent compressive strain was monitored in all cross-sections of the surrounding concrete, and the compressive strain was from -50 με to -100 με. The

Table 3 Comparison of the measured strain (unit: με)

Cross-section	Position	Sensing cable	Reinforcement gauge	Strain gauge
Hc1	top	-53	-11	none
	mid	-99	-41	-11
Hc3	top	-66	-9	none
	mid	-64	-46	-65

internal stress of concrete structure adjusted during unloading. However, the change of measured strain was small. The average hoop compressive strain was about -70 με on top of each cross-section, and about -100 με at the middle after unloading. The compressive strain at the middle of surrounding concrete was 30 με larger than that on top during unloading. It may be explained that the direction of the hoop strain at the middle is vertical, and horizontal on top. The vertical compressive stress at the middle will increase more because of the gravity of concrete itself after decompressing.

5.2 Comparison with reinforcement gauge and strain gauge

Reinforcement gauges were installed at the top, middle and bottom of four monitoring cross-sections, and five-direction strain gauges were embedded at the middle and bottom of the cross-sections. Take the measured strain before decompression as a reference value, the strain variation was calculated and compared with that of adjacent sensing cables. The characteristics of measurement on each cross-sections were close, as shown in table 3.

The measurement of concrete strain gauge was discrete and half of the gauges did not work normally. Without consideration of obvious abnormalities, the average strain change during decompression was -51 με, which is less than that measured by sensing cable.

The measured strain by reinforcement gauge was stable. However, the strain was generally smaller than cable strain.

The measured compressive strain by reinforcement gauge was about 32% of that by sensing cable. With the consideration the coordinate deformation between of rebar and concrete, the above phenomenon can be explained that the compressive strain measured by sensing cable was more accurate because the cable have low modulus and good flexibility. For the reinforcement gauge, due to its large volume and stiffness as well as the residual strains formed by welding or installation, it may be hard to measure the small compressive strain accurately.

5.3 Gap width between spiral case and surrounding concrete

When the concrete was poured with the preloading of the spiral case, there forms the initial gap between the spiral case and the surrounding concrete. The gap width is mainly controlled by the preloading pressure. For large turbine, the width is also affected by the temperature. In the design of the spiral case, the following two aspects are considered for preloading pressure. One is the load sharing proportion between the spiral case and the surrounding concrete. The trend is to decrease the load on the concrete structure as much as possible to reduce the reinforcement ratio and the construction cost. The other is to ensure a close contact between the spiral case and surrounding concrete when the turbine works under the lowest water pressure. In addition, the spiral case and the axis of the turbine will not shift because of the pressure or vibration of water. Due to the lack of convincible measured data, the structure load under different working conditions could only be obtained by calculating the initial gap width of different cross-sections in current design.

A reliable and large-scale BOTDA-based strain distribution was obtained in this test, which will be for the reference of designers. Especially, the surrounding concrete shrinkage was observed during the decompression, which indicates that the initial gap may decrease.

The gap width was estimated by using the following formula

$$d = (\varepsilon_1 - \varepsilon_2) \times r \times 10^{-3} \tag{5}$$

where ε_1 and ε_2 are the strain change of the surrounding concrete and spiral steel case. The average strain of ε_1 and ε_2 were -70 με and -370 με respectively; *r* is the radius of spiral case. For Gc3~Gc7 cross-section, the radius (r) are 2.5~1.7 m. The calculated gap width were 0.75~0.51 mm. It should be noted that the width was only estimated for the radial shrinking to the center of a circle. The actual situation was more complex, and the width may be slightly different.

6. Conclusions

High-performance BOTDA instruments and specified strain sensing cables were adopted to monitor the loaded spiral steel case and the surrounding concrete of the 4 # turbine in JinPing-II hydropower station. Conclusions are as follows according to the monitored data of the cross-sections.

The strain distribution of each cross-section was consistent, and had a good correlation with the pressure changes during water-filling test of spiral case. The strain on the mid piece of spiral case was larger than that of top and bottom pieces. The strain measured by using sensing cable was close to the value of theoretical formula and numerical simulation. The difference was only about 50 με.

During the unloading process, the strain of sensing cables in each cross-sections of the surrounding concrete was close. The average hoop compressive strain was about 70 με on top of spiral case, and about 100 με at the middle after unloading. The strain obtained by concrete strain gauges and reinforcement gauges showed the same rules except that their strain was significantly smaller than the measurement of sensing cables. According to the average strain of -370 με on the spiral case surface, the average gap width between the spiral case and surrounding concrete from Gc3 to Gc7 was 0.51~0.75 mm after unloading with assumption of the radial shrinking to the center of a circle.

According to test results, the distributed optical fiber sensor is better than the traditional point sensor. The survival rate and reliability of the point sensors was relatively low because it is difficult to install the steel plate stress meter and concrete strain gauge. The survival rate of the reinforcement gauge was relatively high, but it may not be possible to accurately capture the small strain change, especially the initial compressive strain below 100 με due to the large rigidity and the welding technics.

It is the first application of distributed optical fiber sensing technology for the monitoring of spiral case, a kind of complicated hydraulic project including steel structure and concrete structure. The reliable data and the monitoring results obtained by BOTDA was unapproachable for traditional point sensors in the past. This application can be used as a reference for similar structures.

Acknowledgements

The authors acknowledge the supports of the National Natural Science Foundation of China (No. 41572271) and the Natural Science Foundation of Jiangsu Province (No. BK20161239).

References

Bao, Y., Tang, F.J., Chen, Y.Z., Meng, W.N., Huang, Y. and Chen, G.D. (2016), “Concrete pavement monitoring with PPP-BOTDA distributed strain and crack sensors”, *Smart Struct. Syst.*, **18**(3), 405-423.

Bao, X.Y. and Chen, L. (2012), “Recent progress in distributed fiber optic sensors”, *Sensors*, **12**(7), 8601-8639.

Culverhouse, D., Farahi, F., Pannel, C.N. and Jackson, D.A. (1989), “Potential of stimulated Brillouin scattering as sensing mechanism for distributed temperature sensors”, *Electron. Lett.*, **25**(14), 913-915.

Ding, C.Q. (2011), “Monitoring result after keeping the pressure and temperature in spiral case of left bank house”, *Hydropower Autom. Dam Monit.*, **35**(2), 67-71.

Horiguchi, T., Kurashima, T. and Tateda, M. (1989), “Tensile strain dependence of Brillouin frequency shift in silica optical fibers.” *IEEE Photonics Technol. Lett.*, **1**(5), 107-108.

Kishida, K., Li, C.H., Li, S.B. and Nishiguchi, K. (2004), “Pulsed pre-pump method to achieve centimeter order spatial resolution in Brillouin distributed measuring technique”, *IEICE Tech. Rep. OFT2004-28*, **104**(341), 15-20.

Li, C.H., Tsuda, T. and Sawa, T. Makita, A., Takano, H., Kishida, K., Wu, Z.S., Takeda, N. and Minakuchi, S. (2008), “PPP-BOTDA method to achieve 10cm spatial resolution and 10Hz measuring speed in distributed sensing”, *IEICE Tech. Rep. OFT2008-42*, **108**(245), 39-44.

Li, H., Ou, J. and Zhang, X. (2015), “Research and practice of health monitoring for long-span bridges in the mainland of China”, *Smart Structu. Syst.*, **15**(3), 555-576.

Liu, R.M., Babanajad, S.K., Taylor, T. and Ansari, F. (2015), “Experimental study on structural defect detection by monitoring distributed dynamic strain”, *Smart Mater. Struct.*, **24**, 115038.

Shi, B., Zhang, D. and Zhu, H.H. (2011), “Application of distributed optical fiber strain measurement into geotechnical engineering monitoring”, *Proceedings of the 8th International Workshop on Structural Health Monitoring*, Stanford, USA, September.

Soga, K., Kwan, V., Pelecanos, L., Rui, Y., Schwamb, T., Seo, H. and Wilcock, M. (2015), “The role of distributed sensing in understanding the engineering performance of geotechnical structures”, *Proceedings of the 16th ECSMGE-Geotechnical Engineering for Infrastructure and Development*, Edinburgh, UK, January.

Xue, Y., Cheng, W.B. and Zhang, M. (2012), “Analysis on hydrostatic test of hydraulic turbine spiral case of Nuozhadu hydropower station”, *Yangtze River*, **43**(4), 67-69.

Yamauchi, Y., Guzik, A., Kishida, K. and Li, C.H. (2007), “A study on the stability, reliability, and accuracy of neubrescope-based pipe thinning detection system”, *SHMII-3*, Vancouver, British Columbia, Canada November 13-16.

Zhang, C.S., Chu, W.J., Liu, N., Zhu, Y.S. and Hou, J. (2011), “Laboratory tests and numerical simulations of brittle marble and squeezing schist at Jinping II hydropower station China”, *J. Rock Mech. Geotech. Eng.*, **3**(1), 30-38.

Zhang, D., Cui, H.L. and Shi, B. (2013), “Spatial resolution of DOFS and its calibration methods”, *Opt. Laser. Eng.*, **51**, 335-340.

Zhang, D., Wang, J.C. and Li, B. (2016), “Fatigue characteristics of distributed sensing cables under low cycle elongation”, *Smart Structu. Syst.*, **18**(6), 1203-1215.

BS